Search for new particles at LEP

S.Rosier-Lees (rosier@lapp.in2p3.fr)
LAPP (IN2P3-CNRS)
Annecy-Le-Vieux - France

Abstract

The LEP energy upgrade up to $\sqrt{\mathrm{s}}$ =189 GeV has allowed to extend substantially the potential of searches for new physics. Results on searches for Higgs bosons and supersymmetric particles obtained by the ALEPH, DELPHI, L3 and OPAL experiments are reported. No evidence of any signal is observed. Therefore new limits on the Higgs boson masses as well as on the masses of the various supersymmetric particles are derived. They significantly improve those obtained either at LEP1 or LEP1.5. The LEP200 discovery potential for the neutral Higgs bosons is also shown

1 Introduction

A wide range of searches for new particles has been performed at LEP and no deviation with respect to the Standard Model predictions was observed yet, unfortunately. Therefore new limits on the masses of these particles, assuming different models, are set by the various experiments. In what follows, all the presented limits are derived at 95 % C.L.. We present first the results of Higgs searches, which are interpreted in the framework of the standard and Minimal Supersymmetric Models. Then the searches for supersymmetric particles are reviewed. In latter case, results are interpreted within Supersymmetric Models like gravity SUSY breaking models or gauge mediated SUSY breaking models. After collecting $\sim 150\,\mathrm{pb}^{-1}$ at LEP1 (1989 $\rightarrow$ 1995), each experiment (ALEPH, DELPHI, L3, OPAL) has accumulated data at LEP2: $\sim$ 5.5 pb^{-1} at $\sqrt{s}$ = 133 GeV (1995), $\sim 10\,\mathrm{pb}^{-1}$ at $\sqrt{s} = 161$ GeV (1996), $\sim 10\,\mathrm{pb}^{-1}$ at $\sqrt{s} = 172$ GeV (1996) and $\sim 55\,\mathrm{pb}^{-1}$ at $\sqrt{s}$ = 183 GeV (1997). This year, an amount of $\sim$ 175 pb^{-1} at $\sqrt{s}$ = 189 GeV (November 1998) is already recorded by each experiment, but the results including all the statistics for 1998 are not yet available; a fraction of the overall integrated luminosity is only used corresponding to the statistics collected just before the summer conference time (up to July 1998 : $30 - 40$ pb^{-1}).

2 The Higgs bosons

2.1 The Standard Model Higgs Boson

The search for the Standard Model Higgs boson is presently only performed at LEP. The current experimental lower limit for it mass m_H, obtained from large samples of

Z boson decays at LEP1 is 63.9 GeV/c^2 as reported in [2]. The accurate electroweak measurements, sensitive to the Higgs mass via the radiative corrections, exclude at 95 % C.L. a Higgs boson heavier than 280 GeV/c^2 [1].
At LEP, the Higgs boson is expected to be produced through the "Higgs-strahlung" process $e^+e^- \rightarrow ZH$, the $e^+e^- \rightarrow WW$ and $e^+e^- \rightarrow ZZ$ contributions being still negligible at those centre-of-mass of energies. For a Higgs mass of 85 GeV, an amount of $\sim$ 20 events is expected per experiment at $\sqrt{s}$=183 GeV.
The background sources are distributed into three subsamples: the $\gamma\gamma$ interactions, the four fermion processes including in particular the WW, Weν, ZZ final states and the two fermion processes. The environments at LEP1 and LEP2 are different as summarized below:

- the fraction $\frac{\text{Signal(HZ)}}{\text{background}}$ increases from 10^{-6} at LEP1 to $\sim 10^{-2}$ at LEP2 as both the Higgs boson production cross section increases and ,above all, the main background from $e^+e^- \rightarrow Z \rightarrow q\bar{q}$ decreases by a factor three in magnitude, allowing to search for Higgs boson through all the possible channels including the four jets channel.
- for $M_H < \sqrt{s} - M_Z$, on shell Z boson are produced. This is an additional constraint very useful for the background rejection.
- However, compared to LEP1, background sources arising from the four fermion processes become more important, bringing in new irreducible background contaminations to the HZ search.

In this new context, the strategy for the Higgs boson searches changed compared to what was performed at LEP1. This search consists of four different channels, determined by the Higgs decay channels together with the Z decay channels. They are presented hereafter sorted according to their branching ratio.
"The four jet channel" : $e^+e^- \rightarrow HZ \rightarrow b\bar{b}b\bar{b}$ is produced with the highest rate ($\sim$ 60%). The signal in this channel consists in four hadronic jets, b flavoured, is the signature for this channel. The key point for this topology is the b-tagging technic which allows to eliminate most of the background arising from $e^+e^- \rightarrow q\bar{q}$,WW and ZZ. In addition the invariant mass of two of the four jets has to be consistent with the Z boson mass.
The "missing energy channel" due to the reaction $e^+e^- \rightarrow HZ \rightarrow b\bar{b}\nu\bar{\nu}$ is characterized by a large missing energy and acoplanar b jets. The best hermeticity and an effective b-tagging are required in order to reduce the background arising from Weν or WW (through W semileptonic decay). This channel is useful due to the relative high branching fraction ($\sim$ 17 %) and the good sensitivity achieved.
The " tau channel" $e^+e^- \rightarrow HZ \rightarrow q\bar{q}\tau^+\tau^-$ in which two isolated taus and two jets are required in the final state. It represents $\sim$ 9 % of the overall decays.
The "electron and muon channels" from $e^+e^- \rightarrow HZ \rightarrow q\bar{q}e^+e^-, q\bar{q}\mu^+\mu^-$ provide a clean signal consisting of two isolated leptons with an invariant mass equal to m$_Z$. With this channel, the best resolution on the Higgs mass is achieved ($\sim$ 2 %) as the well as the best sensitivity. Unfortunately, the branching fraction is low and is equal to 6 %.

The typical overall signal efficiency reached is of the order of 30 % for an expectation of 6 to 11 events from standard processes; no excess in any channel for any experiment is observed, as illustrated on the mass distribution of the candidate events observed by the OPAL experiment (Fig.1). The agreement between the observation and the Standard Model expectations allowed to extract a limit on the Higgs boson mass. The ranges of the limits obtained by each experiment are listed in Tab. 1. Since the limit results do not reach the kinematic limit, more luminosity will be useful. Therefore, in the framework of the LEP Higgs Working Group [3], an effort has be done to combine the results of the four LEP experiments. The combination leads to a gain of about 3–4 GeV with respect to the individual experiments. The 95 % confidence level upper limit obtained for each statistical method is shown on Fig.2 as a function of the Higgs mass. The four different combinations all agree within a spread of $\pm$ 0.15 GeV; conservatively the lowest limit (method C) is quoted in Tab. 1; It has to be noticed that the limits have been improved, for each LEP experiment, by almost 4 GeV/c^2 with the recent data collected at 189 GeV [11], reaching therefore the level of the combined limit at 183 GeV. In reference [4], prospect studies show that Higgs boson with a mass up to 107 GeV/c^2 could be discovered at LEP200 when running at $\sqrt{s}$=200 GeV and assuming an integrated luminosity of 200 pb^{-1} collected by each experiment.

	$M_{H_{SM}}$ lower limit (GeV/c^2)	
	Range of Individual Limit (ADLO)	lower LEP combined
H (Obs.)	**85.7–88.3**	**89.8**
(Exp.)	85.0–86.5	90.4

Table 1: Individual and LEP combined Observed and expected mass limits for the Standard Model Higgs boson [3], up to $\sqrt{s}$ = 183 GeV

2.2 The MSSM Higgs bosons

In the MSSM, all SUSY particle masses, their couplings and their production cross sections and decay widths are predicted in terms of only six free independent parameters: $m_{1/2}$ (the common gaugino mass parameter at the GUT scale), m_0 (the common mass for scalar fermions at the GUT scale), μ (the higgsino mixing parameter), tanβ (the ratio of the vacuum expectation values of the two Higgs doublets), m_A (the mass of the neutral CP-odd Higgs boson A) and A(the trilinear coupling in the Higgs sector at the GUT scale); the renormalization group equations are used to determine the parameters at low energies. Instead of $m_{1/2}$, the LEP experiments usually derive their results as a function of the parameter M_2, the SUSY breaking mass term associated with the SU(2)$_L$ gauge group ($m_{1/2} \approx M_2/0.81$).

Presently, only the lightest neutral Higgs bosons h and A can be discovered at LEP2 [2], since the CP–even Higgs boson H and the charged Higgs bosons $H^{\pm}$ are expected to be

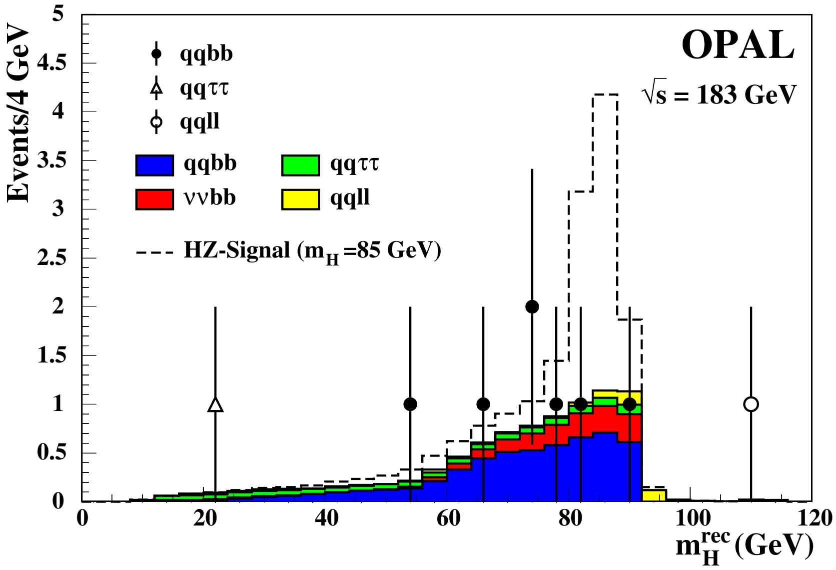

Figure 1: Mass distribution for the candidate events selected by the OPAL experiment in the searches for $e^+e^- \to HZ$ at center-of-mass energies up to 183 GeV [3]

too heavy. However searches for charged Higgs bosons are also performed at LEP2 in the framework of a non–SUSY two–Higgs doublet model.

The lightest neutral Higgs bosons

The lightest neutral Higgs bosons (h and A) could be observed at LEP through the two following processes:

- The Standard Model–like Higgs–strahlung process, $e^+e^- \to hZ$; the cross section for this process is equal to its SM analogue, reduced by a factor $\sin^2(\alpha - \beta)$ which means that this process occurs mainly at low tanβ values.
- The associated pair production process, $e^+e^- \to hA$, with a cross section proportional to $\cos^2(\beta - \alpha)$; this process is dominant at large tanβ values.

In the first channel, searches are similar to those performed for the SM Higgs boson. For tanβ >1 the main decay modes of the h and A bosons are into $b\bar{b}$, and to a lesser extent $\tau^+\tau^-$. Most of the experimental analyses required therefore at least two b quarks in the final states, as detailed in Tab. 2. Clearly, b–tagging plays a crucial role in all the Higgs searches at LEP; it allows to reach very high sensitivities by rejecting most of the WW background. Peculiar decays such as $h \to AA$ or $h \to \chi_1^0\chi_1^0$ have been also considered; the sensitivities achieved in the latter case are better compared to those obtained with the standard decay channels at LEP1 but worse at LEP2. Typical efficiencies and background expectations are listed in Tab. 3, where observation and expectation from SM processes agree very well.

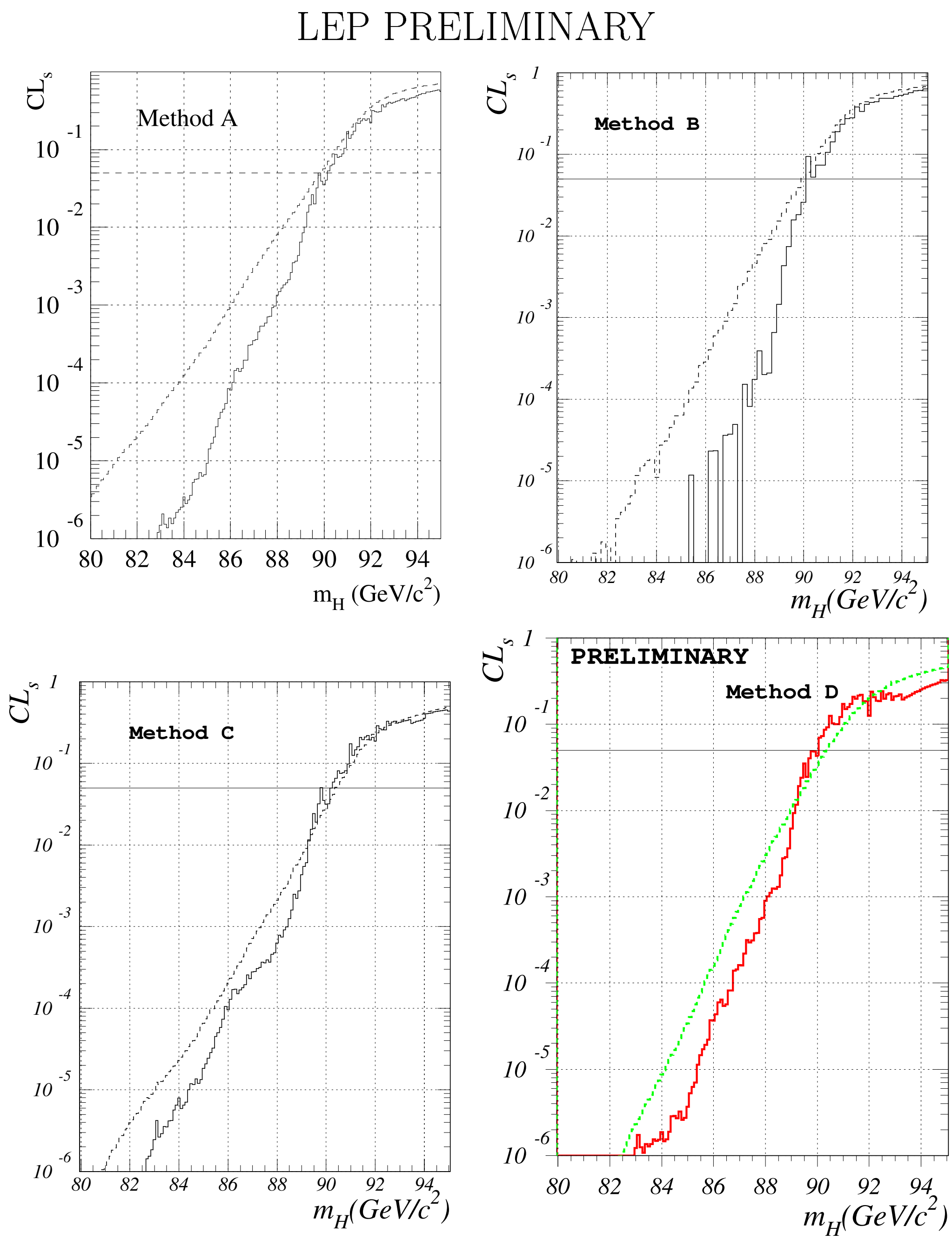

Figure 2: *Average expected (dashed lines) and observed (solid lines) confidence levels, CL_s, obtained from combining the results of the four LEP Collaborations using the four statistical methods. The intersections of the curves with the horizontal lines at 0.05 define the 95% confidence level lower bounds, expected and observed, for the mass of the SM Higgs boson.*

Therefore, limits have been extracted [5]– [10], for two "benchmark" sets of the MSSM parameters where M_{susy}, representing the stop mass mean value is fixed to 1 TeV and $m_t = 175$ GeV, as shown in Figs. 3; M_A varies up to 2 TeV and tanβ from 0.5 to 50, and either minimal or no stop mixing [$A = 0$ TeV, $\mu = -0.1$ TeV] or maximal squark mixing [$A = \sqrt{6}$ TeV, $\mu = -0.1$ TeV] is assumed.

$\sqrt{s}$ (GeV)	hA	hZ
161,172,183	hA$\rightarrow$ b$\bar{\text{b}}$b$\bar{\text{b}}$	Zh$\rightarrow$ $\nu\bar{\nu}$(h $\rightarrow$ all)
	hA$\rightarrow$ b$\bar{\text{b}}\tau^-\tau^+, \tau^-\tau^+$ b$\bar{\text{b}}$	Zh$\rightarrow$ l$^-$l$^+$(h $\rightarrow$ all)
	AAA$\rightarrow$ b$\bar{\text{b}}$b$\bar{\text{b}}$b$\bar{\text{b}}$	Zh$\rightarrow$ $\tau^-\tau^+$(h $\rightarrow$ all)
		Zh$\rightarrow$ (h $\rightarrow$ all) $\tau^-\tau^+$
		Zh$\rightarrow$ q$\bar{\text{q}}$b$\bar{\text{b}}$
		Zh$\rightarrow$ q$\bar{\text{q}}$ or $l^-l^+(h \rightarrow \chi_1^0\ \chi_1^0)$

Table 2: Search channels for the neutral Higgs bosons at LEP.

The limits obtained by each experiments within these assumptions are listed in Tab. 4. The combined limit, obtained as described in Ref. [3] leads to a gain of about 3–4 GeV with respect to the individual experiments. All the methods used for the combination agree within a spread of $\pm$ 1.9 GeV; conservatively the lowest limit is quoted in Tab. 4 (method C of Ref. [3]), while the highest limits (with method D) are given in Figs. 3. These limits are valid for tanβ greater than 0.8, irrespectively of the mixing value or of the method used for the combination. For the no mixing scenario, the range of tanβ between 0.8 and 2.1 is excluded independently of the method. It has to be noticed that the limits have been improved, for each LEP experiment, by almost 4 GeV/c^2 with the recent data collected at 189 GeV [11], reaching therefore the level of the combined limit at 183 GeV. It has been pointed out recently in Refs. [10], [8], [6], that selected sets of the MSSM parameters lead to less stringent exclusions, either because of an unexpectedly small bremsstrahlung cross section or because of a reduced decay branching ratio into $b\bar{b}$. The theoretical status of these pathological parameter sets is currently under investigation. Meanwhile, the limits obtained in the benchmark cases can be regarded as sufficiently robust for practical purposes as demonstrated in Ref. [6].

The charged Higgs Boson

The $H^{\pm}$ bosons can be produced in e^+e^- interactions via the process $e^+e^- \rightarrow \gamma^*, Z^* \rightarrow H^+H^-$ and are expected to decay mainly into the heaviest lepton kinematically allowed and its associated neutrino, or into the heaviest kinematically allowed quark pair whose decay widths are not Cabibbo suppressed; the relative branching ratios are model dependent. Therefore searches are performed in the three possible decay modes: $e^+e^- \rightarrow H^+H^- \rightarrow \tau^-\bar{\nu}_\tau\tau^+\nu_\tau$, $\tau^+\nu_\tau s\bar{c}$ and $c\bar{s}s\bar{c}$. For each experiment [13]– [16] and each decay channel, the number of selected events in the data is consistent, with the number of expected events from SM processes, as can be seen in Tab. 5. Compared to the neutral Higgs boson searches, the sensitivities achieved are lower; this is due to the high WW background contamination. The 95 % C.L. individual limits on the charged Higgs boson

Selection	ϵ(%) for hZ M_h=80 GeV/c^2	N^{exp}_{signal}	N^{exp}_{Bkg}	N^{obs}
hl^+l^-	78.3	1.1	2	3
$h\nu\bar{\nu}$	20.9	0.8	0.16	0
$b\bar{b}q\bar{q}$	23.6	3.6	1.4	1
$b\bar{b}\tau^+\tau^-$	22.7	0.14	0.17	0
$\tau^+\tau^- q\bar{q}$	9.8	0.16	0.16	0
Selection	ϵ(%) for hA $M_h = M_A$=75 GeV/c^2	N^{exp}_{signal}	N^{exp}_{Bkg}	N^{obs}
$b\bar{b}b\bar{b}$	60.5	3.1	2.4	2
$b\bar{b}\tau^+\tau^-$	28.6	0.27	0.07	0

Table 3: Typical efficiencies and expected/observed number of events for the neutral Higgs bosons searches performed by the ALEPH experiment [5] at $\sqrt{s}$=183 GeV.

	$M_{h,A}$ lower limit (GeV/c^2)	
	Range of Individual Limit (ADLO)	lower LEP combined
h (Obs.)	**70.7–74.4**	**78.8**
(Exp.)	67.4–70.3	76.3
A (Obs.)	**71.0–76.1**	**79.1**
(Exp.)	68.4–72.0	76.3

Table 4: Individual and LEP combined mass limits for the neutral h and A bosons [3].

$M_{H^\pm}$=60 GeV/c^2	$\tau^+\bar{\nu}_\tau\tau^+\nu_\tau$	$\tau^+\nu_\tau s\bar{c}$	$c\bar{s}s\bar{c}$
Efficiency	24 %	42 %	40 %
Expected events	9.2	30.1	99.4
Observed events	6	28	93

Table 5: Typical efficiencies, number of expected and observed events obtained by the L3 experiment in the charged Higgs boson searches at c.m. energy of 183 GeV [15].

	$M_{H^\pm}$ Lower limit (GeV/c^2)	
	Range of Individual Limit (ADLO)	Lower LEP combined
$\mathbf{H^\pm}$ (Obs.)	**56.6–59.0**	**68.0**
(Exp.)	56.0–62.0	69.0

Table 6: Individual and LEP combined mass limits for the charged Higgs bosons.

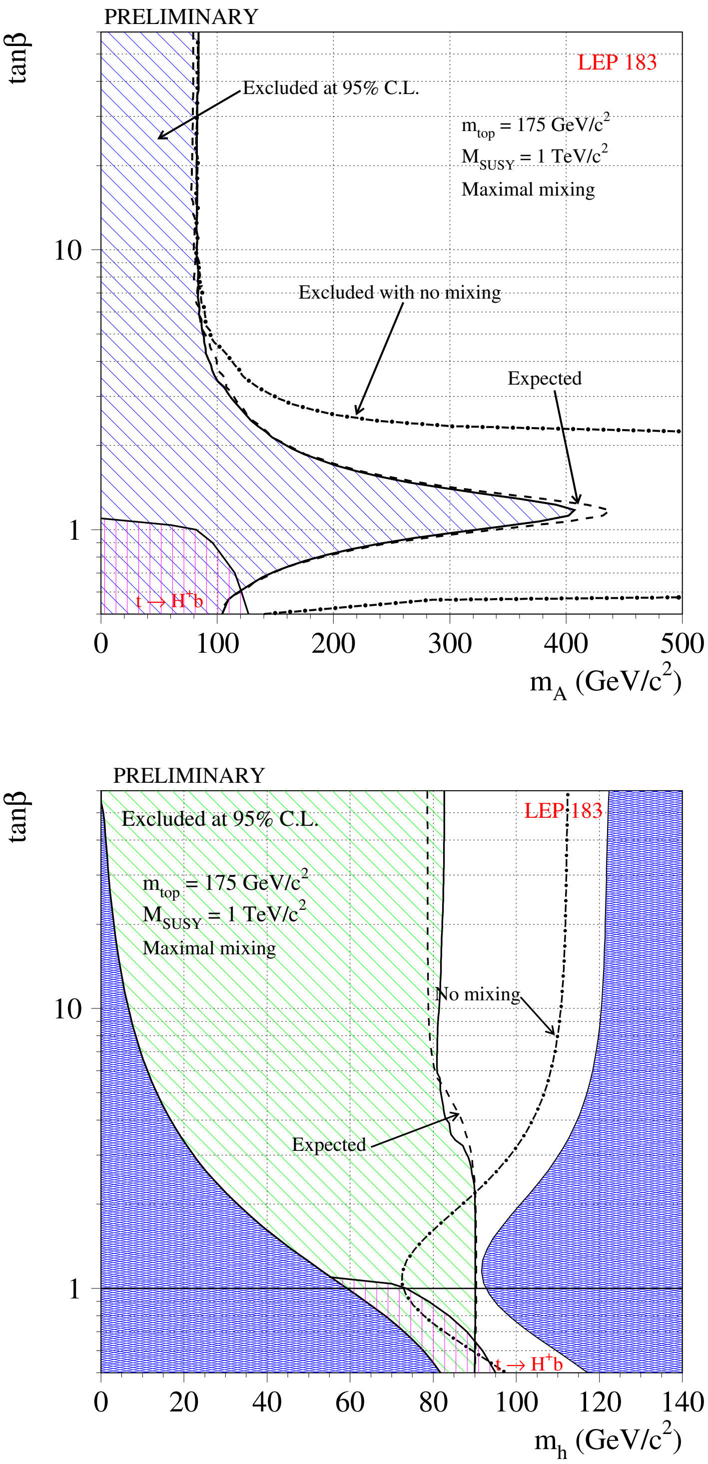

Figure 3: LEP combined exclusion domains (method D) in the plane $(\mathrm{M_A}, \tan\beta\ )$ (top) or $(\mathrm{M_h}, \tan\beta\ )$ (bottom) by the LEP direct searches for $\mathrm{e^+e^-} \rightarrow \mathrm{hZ}$ and hA at center-of-mass energies up to 183 GeV assuming either a maximal mixing or no mixing [3] and [12].

mass is shown as a function of the branching ratio Br($H^{\pm} \rightarrow \tau^{\pm}\nu_{\tau}$) in Fig. 4. Combining all LEP results, a lower limit on the charged Higgs boson mass of 68 GeV is established at the 95 % C.L., assuming that the sum BR($H^{+} \rightarrow \tau^{+}\nu_{\tau}$) + Br($H^{+} \rightarrow c\bar{s}$) is equal to one. It represents a gain of almost 10 GeV with respect to the individual limits, Tab. 6.

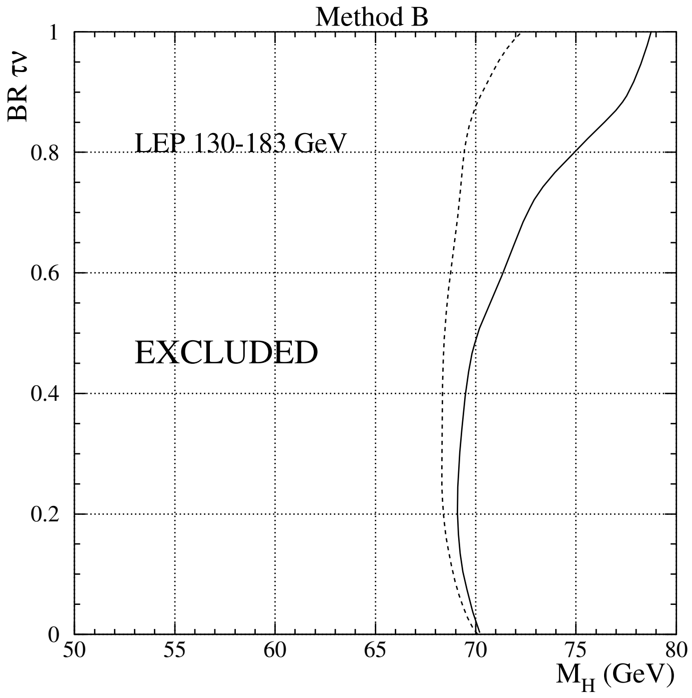

Figure 4: LEP combined exclusion domains in the plane ($M_{H^{\pm}}, Br(\mathrm{H}^{\pm} \rightarrow \tau\nu_{\tau})$) by the LEP direct searches for $\mathrm{e}^{+}\mathrm{e}^{-} \rightarrow \mathrm{H}^{+}\mathrm{H}^{-}$ at center-of-mass energies up to 183 GeV [3].

3 Other SUSY particles

The searches for supersymmetric particles, but the Higgs bosons, at LEP2 concern sleptons, stops, sbottoms, charginos and neutralinos as detailed in [18] and [19]. The most popular SUSY breaking mechanisms are the gravity and the gauge mediated SUSY breaking models (GMSB). The results of SUSY searches at LEP are interpreted in the framework of these two models. In general to avoid lepton and baryon number violations, induced by SUSY loops, the conservation of a new quantum number is invoked: R=(-1)$^{L+2B+2J}$,=1 for standard particles and =-1 for SUSY particles. Within this assumption, the lightest SUSY particle (LSP) is stable and escapes detection since it is supposed to be neutral and weakly interacting. In particular in gravity SUSY breaking models, the LSP is the lightest neutralino ($\tilde{\chi}^{0}_{1}$) while in GMSB models it is the gravitino ($\tilde{\mathrm{G}}$, with $M_{\tilde{\mathrm{G}}} \sim$ 1 eV)

3.1 $\tilde{\chi}_1^0$ LSP scenario

The various pair produced SUSY particles decay to SM particles and LSPs. SUSY signatures consist of some combination of jets or/and leptons and missing energy carried out by the LSP. The signal topology and the background conditions are in practice affected by the SUSY particle and the LSP mass difference ($\Delta M = m_{\mathrm{SUSY}} - m_{\chi_1^0}$) which controls the visible energy. In the low $\Delta M (= 5 - 10$ GeV) range, the expected topologies for the signals are characterized by a low multiplicity and a low visible energy and the background is dominated by two–photon interactions. For large $\Delta M (= 50 - 60$ GeV) values, the signal signatures are very similar to those of W–pair production. Since all the background sources are due to well calculable processes with reasonable production cross sections compared to the signal, most of the decay channels are studied at LEP2.

Scalar leptons

LEP experiments excluded scalar neutrinos with masses up to 43 GeV, from the comparison of the measured Z widths with the SM expectations [20].

In e^+e^- collisions, the production of scalar muons $\tilde{\mu}$, scalar taus $\tilde{\tau}$ proceeds via γ or Z exchange in the s–channel only, whereas scalar electrons $\tilde{e}$ can also be produced by exchanging neutralinos in the t–channel.

The scalar leptons dominantly decay into their SM partners and the lightest neutralino χ_1^0. If the scalar lepton is not the next–to–light SUSY particle (NLSP), cascade decays via χ_2^0 or via the lightest chargino χ_1^+ [for $\tilde{l}_L$ only for a pure gaugino–type chargino] may be possible. The topologies arising from scalar lepton production are then usually, acoplanar leptons plus missing energy. As already explained in the introduction, the sensitivities for these searches depend strongly on the mass difference, $\Delta M, between the scalar lepton and the \chi_1^0$. Typical efficiencies and expected events from SM processes for different ΔM ranges are given in Tab. 7.

$m_{\tilde{l}^\pm} = 75$ GeV									
	$\tilde{e}_R$			$\tilde{\mu}_R$			$\tilde{\tau}_R$		
ΔM (GeV)	ϵ (%)	$N_{\mathrm{sign}}^{\mathrm{exp}}$	$N_{\mathrm{back}}^{\mathrm{exp}}$	ϵ (%)	$N_{\mathrm{sign}}^{\mathrm{exp}}$	$N_{\mathrm{back}}^{\mathrm{exp}}$	ϵ (%)	$N_{\mathrm{sign}}^{\mathrm{exp}}$	$N_{\mathrm{back}}^{\mathrm{exp}}$
75	65	33.8	7.6	66	4.5	6.9	43	2.9	5.9
15	57	7.4	0.5	45	4.3	0.15	38	2.4	3.2
5	11	0.9	0.7	13	0.9	0.9	7	0.5	1.5

Table 7: Scalar electron, scalar muon and scalar tau sensitivities. Results are obtained at $\sqrt{s} = 183$ GeV by the ALEPH experiment [21] as a function of ΔM for $m_{\tilde{l}^\pm} = 75$ GeV.

No excess with respect to the number of events expected from SM processes was observed at LEP up to $\sqrt{s}$=183 GeV [21]– [25]. Since in general, the cross section for the pair production of $\tilde{l}_R$ is smaller than for $\tilde{l}_L$, limits on masses are given by default taking into account $\tilde{l}_L\tilde{l}_R$ production only. The expected background from W–pair production is subtracted for all LEP analyses. All limits are derived in the plane $(m_{\chi_1^0}, m_{\tilde{l}_R})$. These

	$m_{\tilde{l}_R}$ lower limit (GeV/c^2)	
	Individual Limit (ADLO)	LEP combined
$\tilde{e}_R$ (Obs.)	**79–83**	**85**
(Exp.)	78–83	85
$\tilde{\mu}_R$ (Obs.)	**55–62**	**71**
(Exp.)	56–67	75
$\tilde{\tau}_R$ (Obs.)	**45–63**	**75**
(Exp.)	45–56	67

Table 8: Individual and LEP combined mass limits for $\tilde{e}_R$, $\tilde{\mu}_R$, $\tilde{\tau}_R$ up to $\sqrt{s} = 183$ GeV for ΔM greater than 20 GeV, and assuming tanβ $= 2$ and $\mu = -200$ GeV for $\tilde{e}_R$.

limits depend only slightly on μ or tanβ for $\tilde{\mu}_R$ and $\tilde{\tau}_R$, since these parameters may just change their couplings to χ^0_2 [relevant only for low masses of χ^0_1 in the region covered anyway by the χ^+_1 searches] but do not affect their cross section for pair–production. For $\tilde{e}_R$, the production cross section in the χ^0_1 t–channel exchange depends on these parameters. The combined exclusion contours of all LEP analyses [17] up to 183 GeV are shown in Figs. 5. The individual limits are derived for different tanβ values $1.4 \rightarrow 2$, and for $\mu = -200$ GeV.

Since we are far from the kinematical limit, more luminosity helps and a gain ranging from 2 to 10 GeV, depending on the scalar lepton flavor, is obtained in the combination as shown in Tab. 8. We should mention also that the individual limits obtained recently at $\sqrt{s}$=189 GeV with an integrated luminosity of 30–40 pb^{-1} for each experiment reach the level of the LEP combined [up to 183 GeV] limit [17].

Assuming a common scalar lepton mass at the GUT scale, the relation between the masses of right– and left–handed sleptons can be used to combine results of the searches for acoplanar leptons (muons, electrons together) [21] coming from the $\tilde{e}_R\tilde{e}_L$ process when the $\tilde{e}_R$ and the χ^0_1 are mass degenerate (ΔM below 3 GeV). The result is shown in Fig. 5 (bottom right), for tanβ $= 2$ and $\mu = 100$ GeV; this value of μ minimizes the product of cross section times branching fraction for the process $e^+e^- \rightarrow \tilde{e}_R\tilde{e}_L$ with $\tilde{e}_L \rightarrow e\chi^0_1$ for vanishing ΔM. In this case, a scalar lepton mass limit of 65 GeV/c^2 is set independently of ΔM; this limit holds for higher values of tanβ .

Scalar quarks

The squarks of the two first generations should be abundantly produced at the Tevatron which places already limits far above the kinematical reach of LEP2. Due to a large Yukawa coupling, the mass of one of the top squarks can be significantly smaller compared to those of the other scalar quarks; the large mixing between the left and right stops, proportional to m_t, leads to a large splitting of the two mass eigenstates. The lighter stop $\tilde{t}_1$ could be within the discovery range of LEP2. In addition, for large tanβ values ($\gtrsim 30$), the mixing angle in the sbottom sector can also be large and the lighter sbottom $\tilde{b}_1$ could also be within the reach of LEP2.

Stop and sbottom production at LEP proceed via Z/γ exchange in the s–channel; the

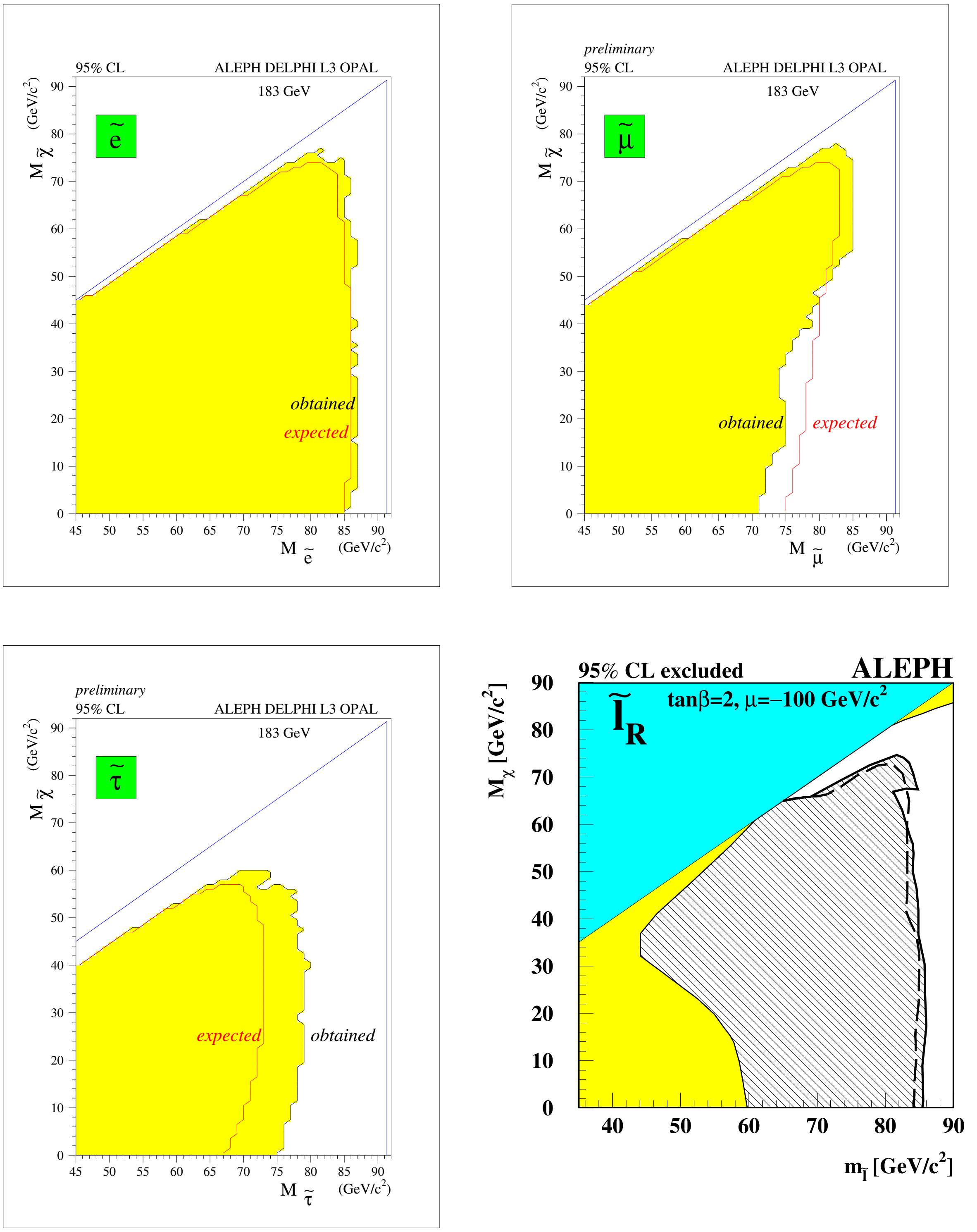

Figure 5: Combined exclusion contours for scalar electrons, muons and taus [17] as a function of the LSP mass and the limit for sleptons obtained by the ALEPH experiment [21] when combining all selectron and smuon searches up to 183 GeV (bottom–right).

production cross sections depend on the squark mass and the squark mixing angle $\cos\theta_q$ and at $\cos\theta_q \sim 0.57(0.39)$ the stop (sbottom) decouples from the Z–boson and the cross section is minimal; the dominant decay modes of the $\tilde{t}_1$ are expected to be $\tilde{t}_1 \to c\chi_1^0$ or $\tilde{t}_1 \to b\tilde{\nu}l^+$; both of these decay modes have been searched for at LEP. The dominant decay mode of $\tilde{b}_1$ is expected to be $\tilde{b}_1 \to b\chi_1^0$.

Under the assumption of R–parity conservation, the χ_1^0 and the $\tilde{\nu}$ are invisible in the detector; thus stop or sbottom pair events are characterized by two acoplanar jets or two acoplanar jets plus two leptons, with missing energy. When the $\tilde{t}_1 \to c\chi_1^0$ decay mode is dominant, the corresponding decay width is small enough for the stop to hadronize into a colorless "stop hadron" before decaying; this feature has been implemented by the LEP experiments in their Monte Carlo programs. No excess of events was observed by any of the four LEP experiments [26]– [29], in the searches for stop and sbottom. Typical sensitivities obtained by the OPAL [29] experiment in the various channels, are listed in Tab. 9. All LEP results have been combined [17] and are summarized in Tab. 10, for ΔM

$m_{\tilde{t}_1,\tilde{b}_1} = 80$ GeV						
	$\tilde{t}_1 \to c\chi_1^0$		$\tilde{b}_1 \to b\chi_1^0$		$\tilde{t}_1 \to bl\tilde{\nu}$	
ΔM (GeV)	ϵ (%)	$N_{\rm back}^{\rm exp}$	ϵ (%)	$N_{\rm back}^{\rm exp}$	ϵ (%)	$N_{\rm back}^{\rm exp}$
7	23	1.97	37	1.97	11.8	1.07
15	58	1.97	61	1.97	64	2.05
80	37	1.97	31	1.97	58	2.05

Table 9: $\tilde{t}_1$ and $\tilde{b}_1$ efficiencies (ϵ) and the number of events expected from the SM ($N_{back}^{\rm exp}$) obtained at $\sqrt{s} = 183$ GeV by OPAL [29] as a function of ΔM for $m_{\tilde{q}} = 80$ GeV.

greater than 15 GeV/c^2. Since a slight lack of events appears for sbottom searches, conservatively, the combination in this channel is done without any background subtraction. The LEP combined excluded regions in the plane $(m_{\chi_1^0}, m_{\tilde{q}})$ are shown in Fig. 6.

Charginos and neutralinos

We now turn to the search for charginos and neutralinos at LEP2. At e^+e^- colliders, charginos $\chi_1^+\chi_1^-$ (neutralinos $\chi_i^0\chi_j^0$ with $i, j = 1, \ldots, 4$ ordered by their masses) are pair–produced via s–channel γ/Z (Z) boson and t–channel sneutrino $\tilde{\nu}$ (selectron $\tilde{e}$) exchange. When the masses of the sfermions are very large, the $\chi_1^\pm$ (χ_j^0 with $j \geq 2$) states decay via an exchange of a virtual W (Z) boson as follows: $\chi_1^\pm \to \chi_1^0 W^* \to \chi_1^0 f\bar{f}'$ ($\chi_j^0 \to \chi_k^0 Z^* \to \chi_k^0 f\bar{f}$ with $k < j$). If the slepton and sneutrino masses are comparable to M_W (M_Z) the charginos (next–to–lightest neutralinos) decay via virtual slepton or sneutrino exchange and the leptonic branching fraction is enhanced. Finally for a slepton or sneutrino lighter than the chargino (next to lightest neutralino), the decay modes $\chi_1^\pm \to \tilde{l}^\pm\nu$ or $l^\pm\tilde{\nu}$ ($\chi_j^0 \to \tilde{l}^\pm l^\mp$ or $\tilde{\nu}\nu$) become dominant. The radiative decays $\chi_j^0 \to \chi_k^0\gamma$ are also possible via higher–order diagrams. For all LEP2 studies, the gluino is supposed to be heavy, otherwise the chargino decay patterns would be different.

	$\mathrm{m}_{\tilde{\mathrm{t}}_1}, \mathrm{m}_{\tilde{\mathrm{b}}_1}$ lower limits (GeV/c^2)	
	Individual Limit (ADLO) or AO only: *	LEP combined **obs** [exp]
$\tilde{t}_1 \to c\chi_1^0$, $\cos\theta_{\mathrm{t}} = 1$	**80–85**	**86** (85)
$\tilde{t}_1 \to c\chi_1^0$, $\cos\theta_{\mathrm{t}} = 0.57$	**72–81**	**83** (80)
$\tilde{t}_1 \to b\tilde{\nu}l$, $\cos\theta_{\mathrm{t}} = 1^*$	**84–85**	**87** (86)
$\tilde{t}_1 \to b\tilde{\nu}l$, $\cos\theta_{\mathrm{t}} = 0.57^*$	**80–82**	**85** (84)
$\tilde{b}_1 \to b\chi_1^0$, $\cos\theta_{\mathrm{b}} = 1$	**78–84**	**86** (83)
$\tilde{b}_1 \to b\chi_1^0$, $\cos\theta_{\mathrm{b}} = 0.39$	**45–68**	**75** (60)

Table 10: Individual and LEP combined mass limits for stop and sbottom up to $\sqrt{s} = 183$ GeV for $\Delta M > 15$ GeV, assuming maximal or minimal production cross sections.

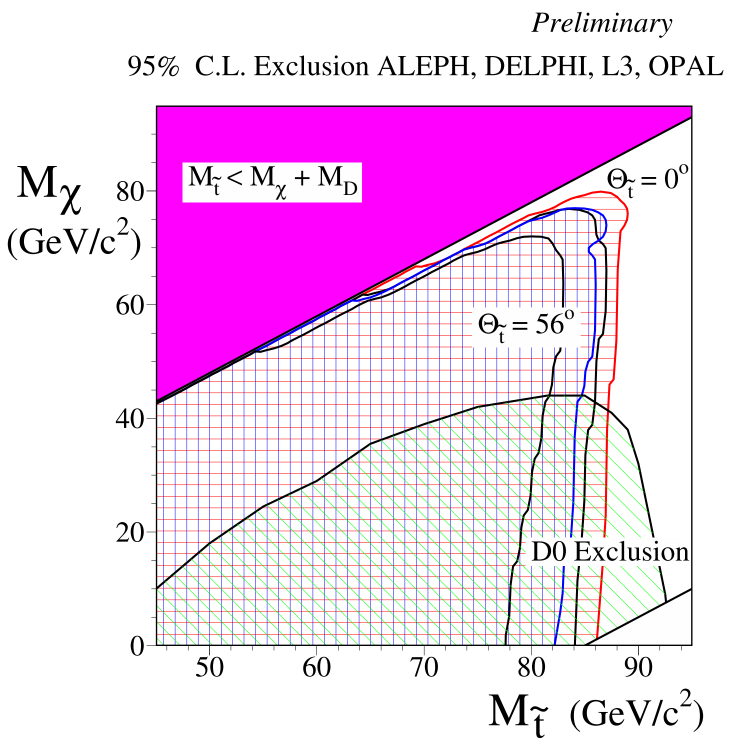

Figure 6: Combined LEP2 [17] exclusion domains in the plane $(m_{\chi_1^0}, m_{\tilde{t}_1})$ from stop decay $\tilde{t}_1 \to c\chi_1^0$ searches. The domain excluded by D0 is superimposed.

The charginos and neutralinos are searched for at LEP2 [31]– [37], in a first time within the large m_0 scenario, i.e large scalar fermion masses. In this case, charginos and neutralinos decay into the LSP accompanied by virtual W and Z bosons. The three possible final state topologies arising from the W and Z decays are: hadrons plus missing energy, acoplanar lepton pairs plus missing energy and mixed final state (hadrons plus leptons) plus missing energy. As explained before, signal topologies and the associated background sources depend on ΔM. Therefore, for each topology, selections were optimized for four different ΔM ranges: the very low (3–5 GeV), the low (5–10 GeV), the medium (20–40 GeV) and the large ($\geq$ 50 GeV). In addition, the DELPHI experiment searched for topologies arising in the very small ΔM regime, with decays in flight and ISR tags [34]. Altogether a total of 27 events was observed by the four experiments with 25$\pm$5 expected from standard processes with efficiencies ranging from 5% to 65% depending on the analysis and the ΔM ranges as illustrated in Tab. 11.

$M_{\chi_1^\pm}$=91 GeV/c^2 $\chi_1^\pm \rightarrow \chi_1^0 W^*$			
ΔM (GeV)	ϵ (%)	$N_{\mathrm{back}}^{\mathrm{exp}}$	N^{obs}
5	15	10.3 $\pm$ 1.1	8
20	55	17.4$\pm$ 1.1	18
60	14	17.4$\pm$1.1	18

Table 11: Typical efficiencies, number of expected and observed events obtained by the DELPHI experiment in the chargino searches at a c.m. energy of 183 GeV [33].

Depending on the neutralino–chargino field content, one distinguishes the following cases for the determination of the lower limits on neutralino–chargino masses:

– Higgsino–like χ_2^0 and $\chi_1^\pm$ ($M_2 \gg |\mu|$): in this case, the production cross sections do not depend on the scalar lepton masses, and ΔM is low and decreases with increasing M_2. Consequently, the limits on the masses of the next–to–lightest neutralino and the lightest chargino decrease with M_2. The present LEP2 combined [17] limit on the chargino mass is shown in Fig. 7 (top left) turning into a limit on the chargino mass of 63 GeV/c^2 for $\Delta M \geq 3$ GeV/c^2 . The DELPHI experiment has excluded regions for lower ΔM ranges as depicted in Fig. 7(bottom). Masses lower than 80 GeV/c^2 are excluded by all LEP experiments for the next–to–lightest neutralino χ_2^0 assuming M_2 less than 1500 GeV/c^2 . This limit holds only for higgsino–like χ_2^0, since the coupling to the Z–boson vanishes for gaugino–like neutralinos.

– Gaugino–like chargino ($|\mu| \gg M_2$): the cross section depends strongly on the scalar neutrino mass. For $50 \leq m_{\tilde{\nu}} \leq 80$ GeV/c^2 the destructive interference term reduces the cross section by one order of magnitude compared to what is expected for $m_{\tilde{\nu}} \geq 300$ GeV/c^2 . When the two body decay $\chi_1^\pm \rightarrow l^\pm \tilde{\nu}$ is dominant, the relevant ΔM becomes equal to $m_{\chi_1^\pm} - m_{\tilde{\nu}}$. Therefore, the limit on the chargino mass will depend clearly on the $m_{\tilde{\nu}}$ value. For large $m_{\tilde{\nu}}$ values ($\geq$ 300 GeV/c^2), the situation is the ideal one: we benefit there from the best detection sensitivity and the highest cross section production. This is the reason why the kinematical limit is reached with only a few pb^{-1} . Up to

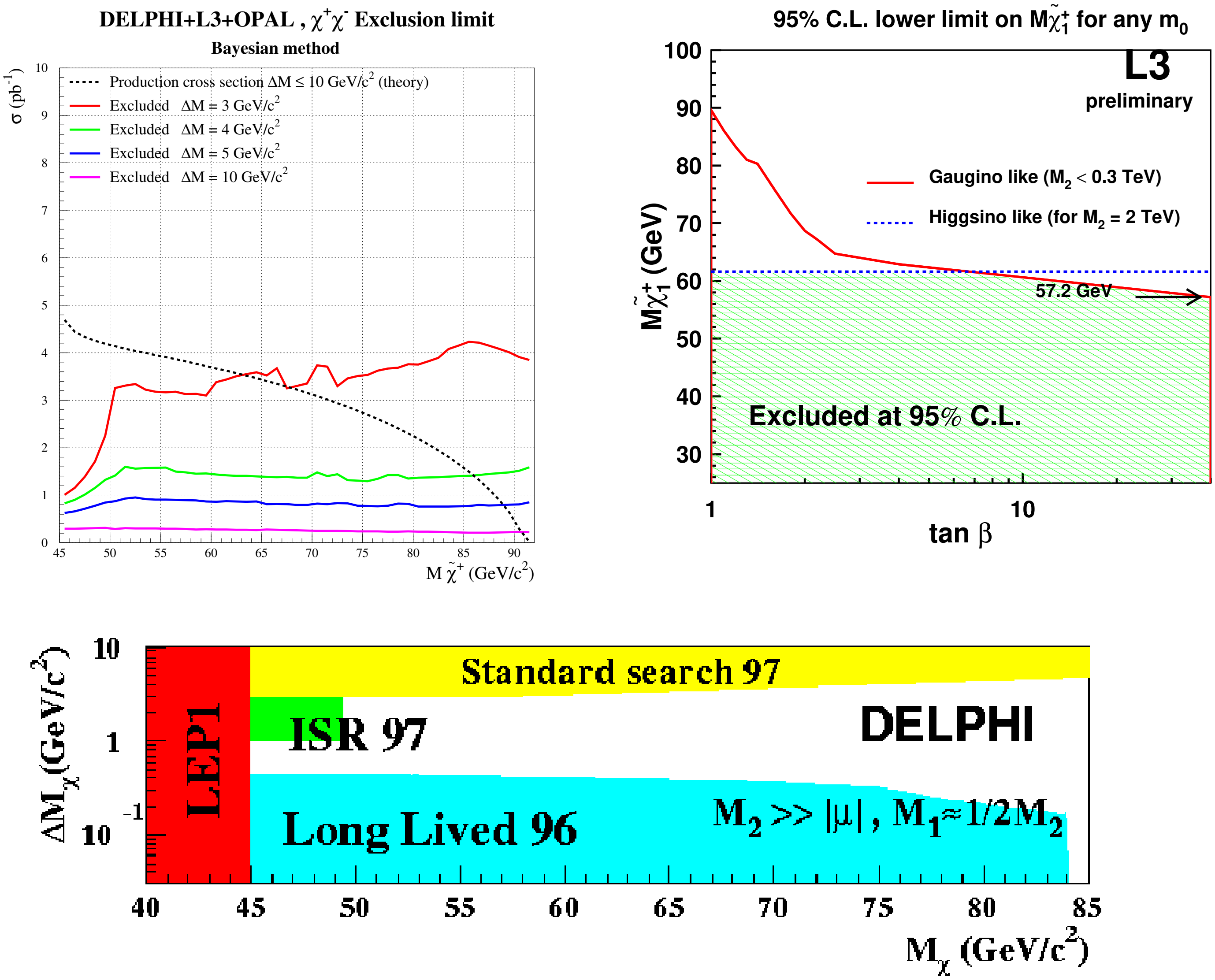

Figure 7: Top left: LEP combined [17] lower limit on the chargino mass for different ΔM values at c.m. energies up to 183 GeV. Top right: lower limit on the chargino mass for different field content, as a function of tanβ , by the L3 experiment [35]. Bottom: excluded domains in the plane $(m_{\chi_1^\pm}, \Delta M)$ in the very low ΔM range obtained by DELPHI [34] at a c.m. energy up to 183 GeV.

now, including the recent 189 GeV data, LEP experiments exclude a chargino mass below 94.3 GeV/c^2, irrespective of tanβ. Extending the study to all $m_{\tilde{\nu}}$ values where the chargino leptonic decay is enhanced for low slepton masses, dedicated analyses were then developed by the LEP experiments. However, it appears that the chargino cannot be directly detected when it is degenerate in mass with the sneutrino since the soft leptons produced in the final state escape detection. In this case, the LEP1 limit of 45 GeV/c^2 remains, that is deduced from the Z–boson total decay width measurement which is insensitive to the chargino decay pattern. Recently, this limit has been improved in two independent ways: (i) the ALEPH experiment, excludes $m_{\chi_1^\pm}$ below 51 GeV/c^2 by measuring the invisible W–boson width, within some model assumptions [32]; and (ii) the L3 experiment [35] exploits the complementarity of the scalar lepton searches, excluding chargino masses below 57.2 GeV/c^2 irrespective of tanβ and m_0, as depicted in Fig. 7 (top right).

Indirect limits on the $\tilde{\chi}_1^0$ mass

Finally, let us discuss the neutralino–LSP mass limits. Since the neutralino χ_1^0 is the LSP and escapes detection, direct searches for the LSP neutralino cannot be performed at LEP2. However, indirect limits have been derived from the constraints on chargino–neutralino and slepton searches. As detailed previously, the limits depend on the slepton masses, in particular on $m_{\tilde{\nu}}$.

– Large sneutrino mass: For high tanβ values, the chargino search provides the most stringent bound on $m_{\tilde{\chi}_1^0}$. For tanβ values below 2, the neutralino searches including the processes $e^+e^- \rightarrow \tilde{\chi}_1^0\tilde{\chi}_3^0, \tilde{\chi}_1^0\tilde{\chi}_4^0$, $\tilde{\chi}_2^0\tilde{\chi}_3^0$ but also the radiative decays $\tilde{\chi}_2^0 \rightarrow \tilde{\chi}_1^0\gamma$, exclude additional regions of the parameter space (mixed region). The LEP1 exclusion limits still play some role, due to the fact that the neutralino search is limited in the region near the point where the χ_1^0 mass limit is set by the value of the coupling to the Z–boson rather than by kinematics. The lower limit obtained for $m_{\chi_1^0}$ as a function of tanβ and for heavy sleptons is displayed in Fig. 8 for LEP center–of–mass energies increasing from 91.5 up to 183 GeV. A summary of all limits [31]– [37] obtained both up to 183 GeV and more recently to 189 GeV is listed in Tab. 12.

– Any sneutrino mass: For lower slepton masses, as already discussed, the constraints in the chargino–neutralino sectors are weaker and the limits on $m_{\chi_1^0}$ is therefore degraded. Constrains on $m_{\chi_1^0}$ have been obtained by all LEP experiments with a systematic scan of the MSSM parameter space, as a function of tanβ for all m_0 values, as depicted in Fig. 8(bottom). For low tanβ values (≤ 1.6) the minimum allowed value for $m_{\chi_1^0}$ is found in the parameter space where the production cross section for charginos is minimal [$m_{\tilde{\nu}} \sim$ 90 GeV/c^2 in the mixed region $\mu \sim -70$ GeV/c^2] [33]– [37] and the heavy neutralino $\chi_{3,4}^0$ are mostly invisible while for higher tanβ values (≥ 2) the lower χ_1^0 mass limit is found in the parameter space region where the chargino and sneutrino mass difference is small and where the next–to–lightest neutralinos χ_2^0 decay invisibly. The exclusion limit came only from slepton searches; it is localized in the deep gaugino–like region for charginos ($\mu \leq -400$ GeV/c^2) [31]. The limits obtained by each experiment are listed

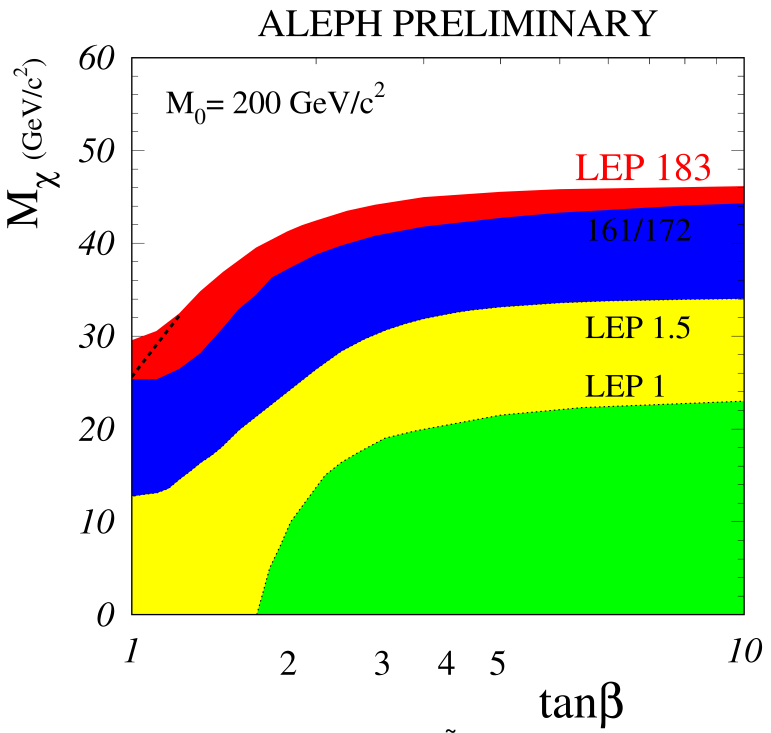

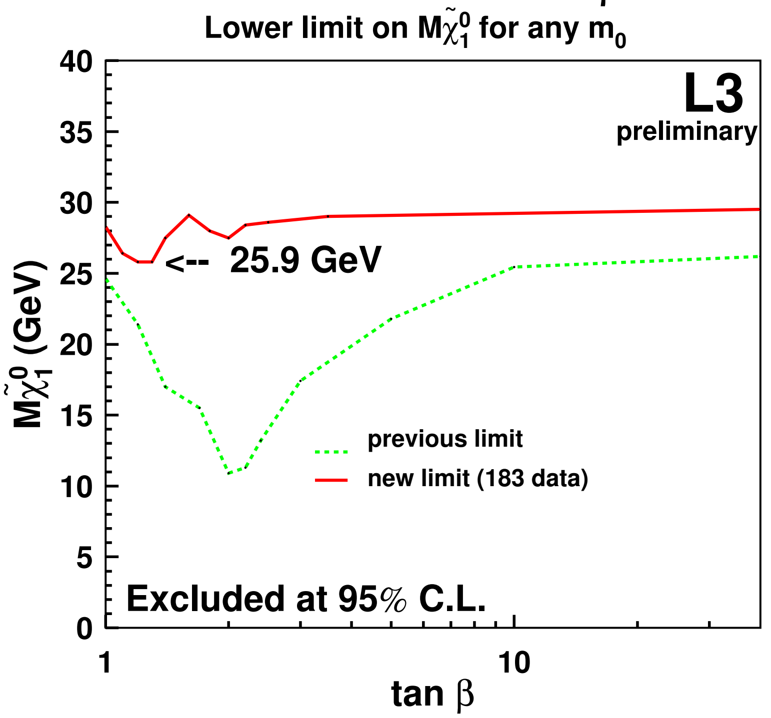

Figure 8: Top: ALEPH [31] lower limit on the LSP mass as a function of tanβ , for large slepton masses, at c.m. energies up to 183 GeV. Bottom: Lower limit on the LSP mass as a function of tanβ , for any slepton mass obtained by L3 [35] at c.m. energies up to 183 GeV

	$m_{\chi_1^0} >$ (GeV/c^2)	
	up to 183 Gev	up to 189 GeV
Large $m_0, \tan\beta \geq 1$	~ 30.5 (ADLO)	~ 32.5 (ADLO)
Any $m_0, \tan\beta \geq 1$		
A μ up to -2000 GeV/c^2	26*	28
D μ up to -200 GeV/c^2	23.4	
L μ up to -500 GeV/c^2	25.9	28.2
O μ up to -500 GeV/c^2	25.4	

Table 12: Indirect individual mass limits for the LSP χ_1^0 up to $\sqrt{s} = 183$, 189 GeV for large m_0 or any m_0. In the latter case, the minimum value (*) for ALEPH experiment is found in the deep–gaugino region (up to 183 GeV data) while other experiments found the minimum in the mixed region.

in Tab. 12 as well as the MSSM parameter ranges used in the scan. The most recent limit on the $\tilde{e}$ mass obtained with 189 GeV data by ALEPH [31] and L3 [36] allows to set the best absolute limit on the LSP mass of ~ 28 GeV/c^2 , which can be turned into an absolute limit on M_2.

3.2 Search for charginos and neutralinos assuming no R–parity conservation

In supersymmetry, R–parity violation can occur through the following Yukawa coupling terms in the superpotential:

$$\lambda_{ijk} L_i L_j \bar{E}_k + \lambda^{'}_{ijk} L_i Q_j \bar{D}_k + \lambda^{''}_{ijk} \bar{U}_i \bar{D}_j \bar{D}_k$$

where L and Q are the SU(2) doublet lepton and quark superfields and E, U, D are the singlet superfields with i,j,k as the generation indices. The simultaneous presence of the last two types of term would induce fast proton decay, which is excluded experimentally. Therefore, it is generally assumed, that among the 45 R–parity violating coupling terms only one (or more generally only one type) dominates. The three types (λ,$\lambda^{'}$,$\lambda^{''}$) have been studied at LEP2.

The main consequence of R–parity violation is that the LSP is no longer stable. The R–parity violating couplings under consideration are strong enough so that the LSP decays within the detector [it requires a strength of the coupling greater than 10^{-3} which is within the existing upper bound obtained from low energy experiments]. The L-violating λ type coupling terms will give rise to multilepton final states, for instance a λ_{ijk} term may induce the decay of a neutralino LSP to final states such as $\bar{\nu}_i l_j^+ l_k^-$ (via virtual slepton or sneutrino exchange) ; the L-violating $\lambda^{'}$ type coupling terms involve multijets with leptons or with some missing energy. Finally, the B-violating $\lambda^{''}$ type coupling terms lead to events with multijets signatures and without missing energy.

In what follows the process involving chargino pair production as well as neutralino pair production ($\tilde{\chi}_1^0\tilde{\chi}_1^0$ but also $\tilde{\chi}_1^0\tilde{\chi}_2^0$) have been studied in which R–parity violation manifests itself only in the decay of the LSP. No signal above the expected standard model backgrounds was detected at LEP [38]- [41] in any of the topologies investigated, resulting into mass limits or constraints on the parameters of the MSSM. As shown by ALEPH on Fig.9 [38], the kinematic limit for the chargino is reached everywhere, in particular in the deep-higgsino region in contrast to the case of R–parity conservation. Assuming a dominant λ_{133} coupling (channel providing the worst sensitivity for this type of coupling), the LEP experiments [39]- [41] have derived a lower limit on the LSP mass equal to 26.8 GeV/c^2 irrespective of tanβ .

3.3 The light gravitino scenario

A class of supersymmetric models in which the gravitino is the lightest supersymmetric particle has recently received renewed attention, since the observation by the CDF experiment [43] of one event containing two electrons, two photons and large transverse missing energy. Within this scenario ($\tilde{\mathrm{G}}$ is the LSP), the phenomenology will depend on the nature of the next to lightest supersymmetric particle. At LEP, one distinguishes two cases: the NLSP is either the lightest neutralino (χ_1^0) or a slepton ($\tilde{\mathrm{l}}$).

χ_1^0 next lightest supersymmetric particle

In such scenario, the lightest neutralino is expected to decay into a photon and a gravitino, $\tilde{\chi}_1^0 \to \gamma\tilde{\mathrm{G}}$. For practical purposes, the neutralino lifetime is negligibly small as soon as the gravitino mass is smaller than a few eV/c^2. In the light gravitino scenario large cross section productions are predicted at LEP2 ($\sim$ 1pb) for the two processes: $e^+e^- \to \tilde{\chi}_1^0\tilde{\chi}_1^0 \to \gamma\gamma\tilde{\mathrm{G}}\tilde{\mathrm{G}}$ and $e^+e^- \to \tilde{\chi}_1^0\tilde{\mathrm{G}} \to \gamma\tilde{\mathrm{G}}\tilde{\mathrm{G}}$ (the latter only for very light $\tilde{\mathrm{G}}$, $M_{\tilde{\mathrm{G}}} \sim 10^{-4}$ eV/c^2). These two reactions lead respectively to the two photon and single photon plus missing energy signatures. For this kind of signatures, there is however an irreducible background due to the reaction $e^+e^- \to \nu\bar{\nu}\gamma(\gamma)$, which should be kept under control.
The combined result obtained by the four LEP experiment is shown in Fig.10 (left), where is displayed the single or two photon recoil mass for data which is in perfect agreement with the SM prediction.
In the single photon channel, upper limits on the production cross section for the process $e^+e^- \to \tilde{\chi}_1^0\tilde{\mathrm{G}}$, have been derived, ranging from 0.1 to 0.7 pb, depending on the analysis and on the mass of the lightest neutralino. In models with superlight gravitinos, the process $e^+e^- \to \tilde{\mathrm{G}}\tilde{\mathrm{G}}$ can be also relevant. When accompanied by initial state radiation this reaction leads to single (or multi) photon signature. $e^+e^- \to \tilde{\chi}_1^0\tilde{\mathrm{G}}$. If $M_{\tilde{\chi}_1^0} \geq \sqrt{s}$, this is the only accessible reaction to produce SUSY particles [42]. In the absence of signal, lower limits on the gravitino mass ranging from 6.6 and 8.8 10^{-6} eV/c^2 have been [44]- [47] set; it can be translated to an upper limit on the SUSY breaking scale $\sqrt{F} \geq$ 182.5 geV.
The two photons final state refers to the pair production of the lightest neutralinos, $e^+e^- \to \tilde{\chi}_1^0\tilde{\chi}_1^0$. The main background from the process $e^+e^- \to \nu\bar{\nu}\gamma\gamma$ is reduced by the requirement that the mass recoiling against the two photons should not be close to the Z boson mass; in addition, a minimum energy for both photons is required. In the absence

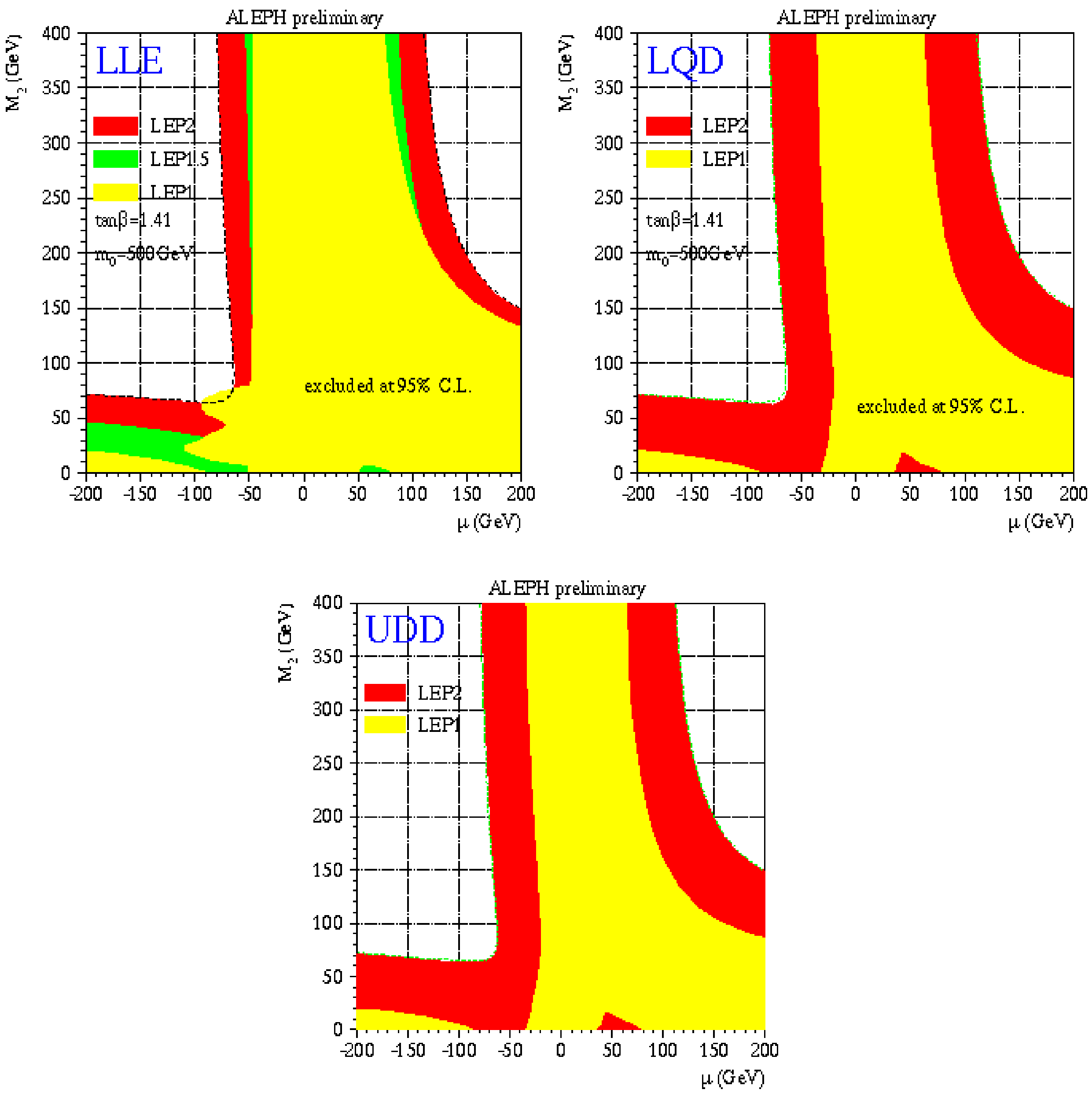

Figure 9: Regions excluded in the (μ,M_2) plane for the three λ type couplings. The dotted line is the chargino kinematic limit

of signal, the LEP combined upper limit on the production cross section of $\tilde{\chi}_1^0$ pairs, reach the level of 0.02-0.04 pb [17]. To turn this constraint into a $\tilde{\chi}_1^0$ mass limit, further model requirements are needed (right or left selectron masses, $\tilde{\chi}_1^0$ field content). Values below 85 GeV/c^2 are typically excluded. Finally, the resulting combined upper limit is confronted with the kinematic region defined by the CDF event. This is shown on Fig. 10(right) where LEP2 data exclude most of the allowed region.

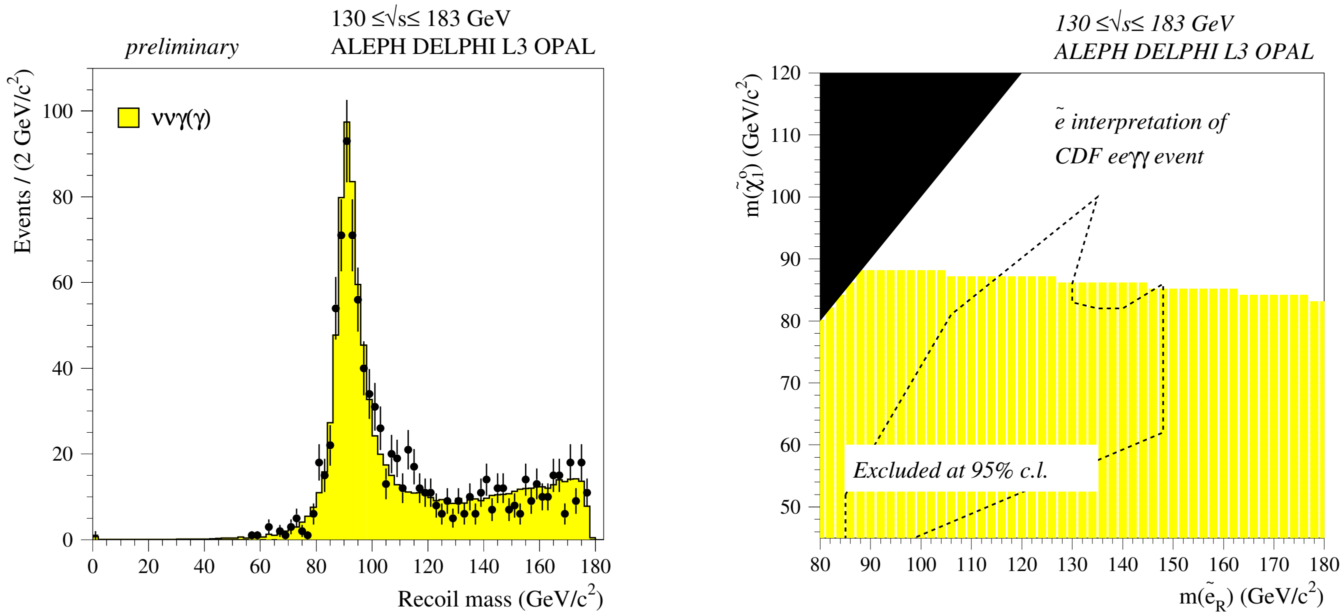

Figure 10: Left: LEP combined recoil mass for single and two photon events [17] Right: The excluded region in the neutralino, selectron mass plane. Overlayed is the region determined from the properties of the event observed by CDF [43].

$\tilde{\mathrm{l}}$ next lightest supersymmetric particle

For a part of the parameter space, the slepton and in particular the stau can be the NLSP, when the gravitino is the LSP; leading to the process:

$$e^+e^- \rightarrow \tilde{\mathrm{l}}^+\tilde{\mathrm{l}}^- \rightarrow l^+l^-\tilde{\mathrm{G}}\tilde{\mathrm{G}}$$

The slepton may decay inside or outside the detector, since the decay length depends on the $\tilde{\mathrm{l}}$ and the $\tilde{\mathrm{G}}$ masses. Three strategies are developed by the experiments depending on this decay length: First, if the decay is prompt, at the interaction vertex, the search is similar to the slepton search in the conventional MSSM, in the limit case of a vanishing neutralino mass. Then for an increasing decay length, one looks for particles decaying into the detector, characterized by events containing tracks with large impact parameters and secondary vertices (kinks). Finally, if the particles decay outside the detector, the particles are seen as heavy stable ionising particles (HIP). The four LEP experiments have

searched for such HIPs; since no excess of events have been observed (two events expected and one candidate event observed) , the LEP combined results, shown on Fig. 11(left), lead to a lower limit on the mass of the $\tilde{\mu}$ (valid also for the $\tilde{\tau}$) equal to 86.5 GeV/c^2 (87 GeV/c^2), depending if the $\tilde{\mu}$ is the supersymmetric partner of the right (left) handed μ respectively.
DELPHI and ALEPH experiments have developed specific analyses for all the different signatures for each lepton flavour. Since no excess of events with respect to the Standard Model expectation has been observed, all the analyses have been combined to derive cross section upper limits which can be turned out in an exclusion contour in the plane $(m_{\tilde{l}}, m_{\tilde{G}})$. For instance, the DELPHI experiment [48] derive a lower limit on the $\tilde{\tau}$ mass of 68 GeV/c^2 irrespective of the mass of the gravitino as illustrated on Fig. 11(right).

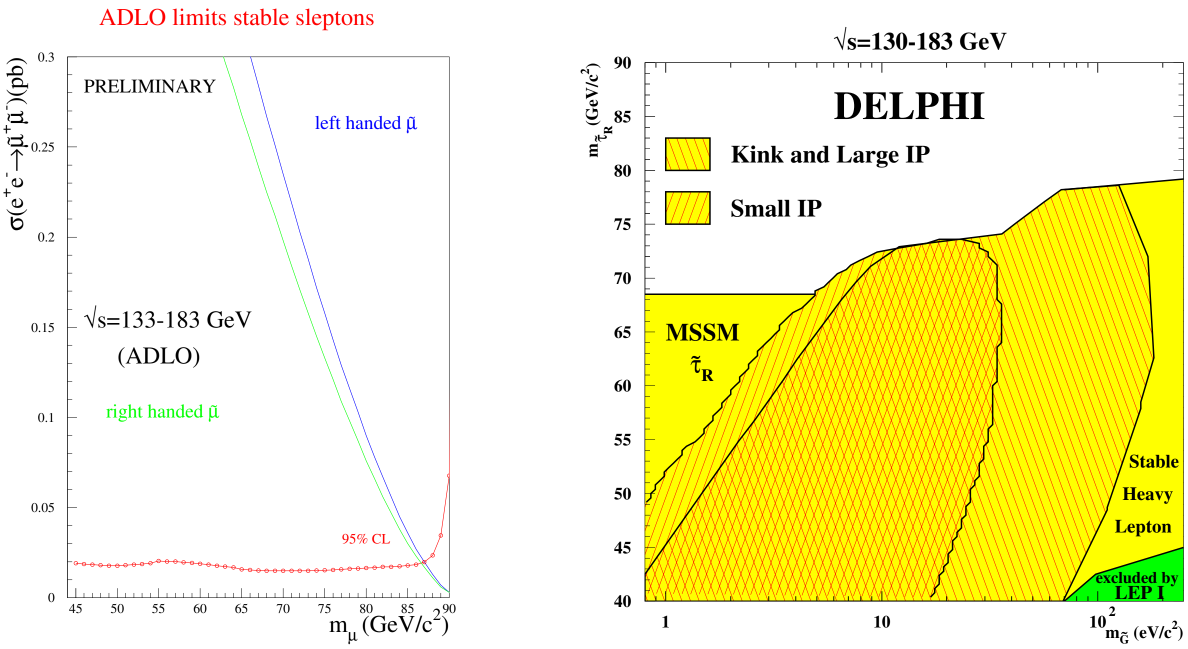

Figure 11: Left: LEP combined upper limit on the production cross section for stable sleptons as a function of the mass of the sleptons. Right: Exclusion region in the $(m_{\tilde{\tau}_R}, m_{\tilde{G}})$ plane by DELPHI. The positive slope hatched area shows the region excluded by the small impact parameter search. The negative slope hatched area shows the region excluded by the combination of the large impact parameter and kink searches.

4 Conclusions and Outlook

A wide variety of searches has been carried out at LEP2 and despite all the efforts, no indication for new physics has been observed yet up to 189 GeV.
Higgs boson searches improve considerably previous results obtained at LEP1 and exclude Higgs masses below 89.8 GeV/c^2 . New limits in the SUSY sector have been derived, in

particular for the neutral Higgs bosons h and A , masses below 77 ,78 GeV/c^2 (respectively) are excluded for tanβ values greater than 0.8. With the coming data foreseen at $\sqrt{s} \sim$ 200 GeV, the SM Higgs with a mass up to 100-110 GeV/c^2 can be discovered at LEP2. LEP2 is also an unique place for SUSY searches: Due to the good detector performances and the relatively good knowledge of the background reactions, a large domain is covered and all channels are exploited. With the absence of any signal, LEP2 excluded chargino masses up to the kinematic limit (94.3 GeV/c^2) for most of the SUSY parameter space and derived an absolute limit equal to 57.2 GeV/c^2 . In addition, an indirect and absolute lower limit, equal to 28 GeV/c^2 , on the Lightest Susy Particle has been derived in the framework of the CMSSM. With future LEP runs, chargino masses up to 100 GeV/c^2 will be explored and a lower mass limit on the LSP of the order of ~ 35 GeV/c^2 will be reached.

Acknowledgements

Preparing such a review needs a lot of discussion and interaction with many colleagues. For this reason I would like to thank Wim deBoer, Laurent Duflot, Alvise Favara, Marta Felcini, Pascal Gay , Paolo Giacomelli, Fabiola Gianotti, Eilam Gross, Peter Igo Kemenes, Patrick Janot, Luc Pape and Pierpaolo Rebecchi from the ALEPH, DELPHI, L3 and OPAL experiments as well as all the members of the Higgs and SUSY LEP working groups for their great help in preparing this talk. I am especially grateful to G.Coignet and J.F Grivaz for the numerous interesting discussions and for a careful reading of the report. It is a pleasure for me to thank the organizers of the SSI for the very stimulating session and for the very pleasant atmosphere at the conference.

References

[1] G. Quast, *Electroweak Physics*, Talk given on behalf of the LEP Electroweak working group, LEPC, 15 sept. 1998. .

[2] P. Janot, *Searching for Higgs bosons at LEP1 and LEP2*, Perpectives on Higgs Physics II, World Scientific Publishing Company, ed G.L. Kane .

[3] The LEP HIGGS Working Group,
Abstract 577-582, ICHEP98, Vancouver, July 1998.
F. Di Lodovico *Report from the LEP Higgs working group*
Talk given on behalf of the LEP HIGGS working group, LEPC, 15 sept. 1998 .

[4] E.Gross et al, *Prospects for the Higgs boson search in Electron-Positron collisions at LEP 200*,CERN-EP/98-094 .

[5] ALEPH collaboration,CERN EP/98-144 Submitted to Physics Letters B .

[6] ALEPH collaboration, Abstract 897, ICHEP98, Vancouver, July 1998 .

[7] DELPHI collaboration, Abstract 200, ICHEP98, Vancouver, July 1998 .

[8] DELPHI collaboration, Abstract 209, ICHEP98, Vancouver, July 1998 .

[9] L3 collaboration, Physics Letters B 436(1998)389-402 .

[10] OPAL collaboration, Abstract 355, ICHEP98, Vancouver, July 1998 .

[11] ALEPH collaboration, Abstract 903, ICHEP98, Vancouver, July 1998 DELPHI collaboration, Abstract 219, ICHEP98, Vancouver, July 1998 L3 collaboration, Abstract 485, ICHEP98, Vancouver, July 1998 OPAL collaboration, Abstract 1069, ICHEP98, Vancouver, July 1998 .

[12] P.Janot, *New Particles Searches*
Talk given at the E.P.S conference in Jerusalem, August 1997 .

[13] ALEPH collaboration, Abstract 900, ICHEP98, Vancouver, July 1998 .

[14] DELPHI collaboration, Abstract 214, ICHEP98, Vancouver, July 1998 .

[15] L3 collaboration, CERN EP/98-161 Submitted to Physics Letters B .

[16] OPAL collaboration, Abstract 1069, ICHEP98, Vancouver, July 1998 .

[17] F. Cerutti *Report from the LEP SUSY working group*
Talk given on behalf of the LEP SUSY working group, LEPC, 15 sept. 1998 .

[18] J.F. Grivaz,*Supersymmetric Particle searches at LEP*, Perpectives on Supersymmetry, World Scientific Publishing Company, ed G.L. Kane .

[19] A.Djouadi, S. Rosier-Lees et al,*The Minimal Supersymmetric Standard Group Summary Report*, http://www.lpm.univ-montp2.fr:7082/ djouadi/GDR/gdr.html .

[20] Particle Data Group, C.Caso et al., *The review of particle Physics* The European Physical Journal C3(1998) .

[21] ALEPH collaboration, Physics Letters B 433,1-2(1998) 176 .

[22] ALEPH collaboration, Abstract 942, ICHEP98, Vancouver, July 1998 .

[23] DELPHI collaboration, Abstract 204, ICHEP98, Vancouver, July 1998 .

[24] L3 collaboration, Abstract 492, ICHEP98, Vancouver, July 1998 .

[25] OPAL collaboration, CERN EP/98-122 submitted to Euro. Phys. Journal C .

[26] ALEPH collaboration, CERN EP/98-076 Submitted to Physics Letters B and Abstract 942, ICHEP98, Vancouver, July 1998 .

[27] DELPHI collaboration, Abstract 204, ICHEP98, Vancouver, July 1998 .

[28] L3 collaboration, CERN EP/98-135 Submitted to Physics Letters B. .

[29] OPAL collaboration, CERN EP/98-107 Accepted by Euro. Phys. Journal C and Abstract 276, ICHEP98, Vancouver, July 1998 .

[30] ALEPH collaboration, Zeitschrift fur Physik c76 (1997)1. .

[31] ALEPH collaboration, Abstracts 942 and 952, ICHEP98, Vancouver, July 1998 .

[32] ALEPH collaboration, Abstract 915, ICHEP98, Vancouver, July 1998 .

[33] DELPHI collaboration, Abstracts 201 and 219, ICHEP98, Vancouver, July 1998 .

[34] DELPHI collaboration, Abstract 202, ICHEP98, Vancouver, July 1998 .

[35] L3 collaboration, Abstracts 485 and 493, ICHEP98, Vancouver, July 1998 .

[36] R. Clare, L3 report to LEPC, November 1998 .

[37] OPAL collaboration, CERN EP/98-136 submitted to Euro. Phys. Journal C and Abstract 273, ICHEP98, Vancouver, July 1998 .

[38] ALEPH collaboration, Abstract 949, ICHEP98, Vancouver, July 1998 .

[39] DELPHI collaboration, Abstracts 210, ICHEP98, Vancouver, July 1998 .

[40] L3 collaboration, Abstracts 496, ICHEP98, Vancouver, July 1998 .

[41] OPAL collaboration, Abstracts 278 and 279, ICHEP98, Vancouver, July 1998 .

[42] A.Brignole et al, Nucl. Phys. B516(1998) 13 .

[43] CDF collaboration, F. Abe et al, FERMILAB-PUB-98-024-E, submitted to Phys. Rev. Lett .

[44] ALEPH collaboration, CERN-EP/98-053, submitted to Physics Letters B .

[45] DELPHI collaboration, Abstracts 206 and 207, ICHEP98, Vancouver, July 1998 .

[46] L3 collaboration, CERN-EP/98-160, submitted to Physics Letters B .

[47] OPAL collaboration, CERN-EP/98-143, submitted to Euro. Phys. Journal C .

[48] DELPHI collaboration, Abstract 205, ICHEP98, Vancouver, July 1998 .